

## Visualizing Multiwavelength Properties of Classified X-ray Sources from Chandra Source Catalog

HUI YANG,<sup>1</sup> JEREMY HARE,<sup>2,3</sup> IGOR VOLKOV,<sup>1</sup> AND OLEG KARGALTSEV<sup>1</sup>

<sup>1</sup>*The George Washington University*

<sup>2</sup>*NASA Goddard Space Flight Center*

<sup>3</sup>*NASA Post-doctoral Program Fellow*

*Keywords:* catalogs – surveys – X-rays

### 1. ABSTRACT

We present a simple but informative online tool to visualize the multiwavelength (MW) properties of  $\approx 2,700$  X-ray sources from Chandra Source Catalog version 2.0 with literature verified classifications. Here we describe the catalogs that we used to collect the classifications and extract the MW properties of these sources, and the properties themselves. We also describe the design and functionality of the tool.

### 2. BACKGROUND

X-ray sources can be classified in a number of different ways. For the brightest sources, one would typically study the X-ray spectrum (e.g., identifying Fe lines, fitting a set of models) and variability properties (e.g., flares, periodicity), in combination with any multiwavelength (MW) counterpart properties. Such comprehensive investigations become unfeasible for the much more numerous population of faint sources lacking high-quality X-ray spectra and light curves. In such cases X-ray properties are less certain and less informative while the MW counterpart properties (e.g., optical colors, X-ray to optical flux ratios) must be more heavily relied upon to classify a given source (see e.g., [Laycock et al. 2005](#); [Clark et al. 2008](#); [DeWitt et al. 2010](#); [Lin et al. 2012](#); [Kargaltsev et al. 2012](#); [Vats & van den Berg 2017](#); [Rivera Sandoval et al. 2018](#); [Tomsick et al. 2020](#)). Collecting the MW properties and being able to visualize them is an important first step.

Chandra Source Catalog 2.0<sup>1</sup> ([Evans et al. 2020](#); hereafter CSC 2.0) contains detailed information about positional, photometric, spectral, and temporal properties for 317,167 unique point and extended X-ray sources. CSC 2.0 is the best catalog for collecting MW properties of X-ray sources located in the Galactic plane due to the sub-arcsecond positional uncertainties<sup>2</sup> (PUs) which result in a much lower chance of confusion when cross-matching.

### 3. SOURCE SAMPLE

We compiled X-ray sources belonging to 9 broad astrophysical classes: active galactic nuclei (AGN), pulsars and isolated neutron stars (NS), non-accreting X-ray binaries (NS BIN)<sup>3</sup>, cataclysmic variables (CV), high mass X-ray binaries (HMXB), low-mass X-ray binaries (LMXB), high mass stars (HM-STAR)<sup>4</sup>, low mass stars (LM-STAR) and young stellar objects (YSO). The classifications were based on the following sources: Veron Catalog of Quasars & AGN 13th Edition ([Véron-Cetty & Véron 2010](#)), the ATNF Pulsar Catalog ([Manchester et al. 2005](#)), the CV Catalog 2006 Edition ([Downes et al. 2001](#)), the HMXB Catalog in the Galaxy 4th Edition ([Liu et al. 2006](#)), the LMXB Catalog 4th Edition ([Liu et al. 2007](#)), the Catalogue of Stellar Spectral Classifications ([Skiff 2014](#)), the VIIth Catalog of Galactic WR Stars ([van der Hucht 2001](#)), the YSO catalogs from multiple molecular clouds and open clusters ([Megeath et al. 2012](#); [Povich et al. 2011](#); [Ozawa et al. 2005](#); [Giardino et al. 2007](#); [Rebull et al. 2011](#); [Delgado et al. 2011](#)).

We cross-matched sources from CSC 2.0 with these catalogs using error circles with the radius equal to the semi-major axis of the  $2\text{-}\sigma$  error ellipse in CSC 2.0. In our cross-matching, we avoided some crowded environments such

Corresponding author: Oleg Kargaltsev  
[kargaltsev@gwu.edu](mailto:kargaltsev@gwu.edu)

<sup>1</sup> <https://cxc.cfa.harvard.edu/csc2/>

<sup>2</sup> <https://cxc.cfa.harvard.edu/csc2/columns/positions.html>

<sup>3</sup> These are wide-orbit binaries with millisecond pulsars, as well as red-back and black widow systems ([Strader et al. 2019](#)).

<sup>4</sup> These include Wolf-Rayet stars.

as globular clusters and the Galactic center as well as sources strongly affected by complex extended emission around them (e.g., bright pulsar wind nebulae). Sources from populous classes (AGN, HM-STAR, LM-STAR and YSO) were omitted if their X-ray PUs were  $> 1''$ . There are several cases of X-ray detected sources from underpopulated classes that are offset by more than  $1''$  from their catalog positions, likely due to poor absolute astrometry. For these sources, we confirmed the classifications/matches by reviewing the literature and inspecting the X-ray and MW images. Finally, we removed unreliable X-ray sources if they had NaNs and/or zero fluxes in multiple X-ray bands or if they had true *sat\_src\_flag* and/or *streak\_src\_flag* in CSC 2.0.

The X-ray sources were then cross-matched, using X-ray error circles, to the optical Gaia eDR3 catalog (Gaia Collaboration et al. 2020), the near-infrared Two Micron All Sky Survey (2MASS; Skrutskie et al. 2006), the CatWISE2020 catalog (Marocco et al. 2021), the unWISE catalog (Schlafly et al. 2019), and the AllWISE catalog (Cutri et al. 2021) in the infrared. For X-ray sources having more than one MW counterpart located within the cross-matching radius, we took the nearest counterpart to the X-ray source as its MW counterpart. We removed unreliable sources such as YSOs or STARS with no matched MW counterparts. We also removed MW counterparts matched with isolated NSs by chance coincidence because virtually all of them are too faint to be detected in those surveys. As a result, we are left with 2,687 X-ray sources. The number of sources for each source class is given at the top of Figure 1.

The visualization tool allows for plotting of various permutations of two of the following features:

- master-level X-ray properties<sup>5</sup> from CSC 2.0 including the energy fluxes in the broad ( $F_b$ ; 0.5-7 keV), hard ( $F_h$ ; 2-7 keV), medium ( $F_m$ ; 1.2-2 keV), and soft ( $F_s$ ; 0.5-1.2 keV) bands, intra-observation Kuiper’s test variability probability ( $P_{intra}$ )<sup>6</sup>, inter-observation variability probability ( $P_{inter}$ ), and X-ray flux significance (Signif.);
- three X-ray hardness ratios derived from the energy fluxes using  $HR_{ms} = (F_m - F_s)/(F_m + F_s)$ ,  $HR_{hm} = (F_h - F_m)/(F_h + F_m)$  and  $HR_{h(ms)} = (F_h - (F_m + F_s))/(F_h + F_m + F_s)$ ;
- $G$ ,  $G_{BP}$  (BP) and  $G_{RP}$  (RP) magnitudes from the Gaia eDR3;
- $J$ ,  $H$ , and  $K$  magnitudes from the 2MASS;
- $W1$  and  $W2$  magnitudes from the CatWISE2020 and the unWISE and  $W3$  magnitude from the AllWISE;
- a selection of colors (e.g.,  $G - J$ ) using various MW magnitudes;
- X-ray to optical flux ratio,  $F_X/F_o$ , with  $F_X = F_b$  and  $F_o$  based on Gaia’s  $G$  band magnitude.

#### 4. THE VISUALIZATION TOOL GUI

The tool, publicly available on a dedicated webpage, <https://home.gwu.edu/~kargaltsev/XCLASS/>, allows for easy interactive plotting of MW properties of the sources for a user-selected subset of source classes. The Graphical User Interface (GUI) is written in Java while plotting is done on-the-fly using the Bokeh Python library<sup>7</sup>. As shown in Figure 1, the user can choose from multiple MW features by clicking the corresponding buttons to the left of the Y-axis and below the X-axis. At the top there are buttons corresponding to the distinct astrophysical classes with the numbers of sources within each class. Users can choose to display different combinations of the classes by toggling/untoggling the class names. Whenever appropriate, a logarithmic scale is used in the plot (which is reflected in the axis labels). The user can select a source by clicking on it and some information about the source will be shown. A *lasso* tool can be used to select a group of sources which then remain selected for any combination of features plotted. The plot can be easily saved as a PNG file by clicking the corresponding button to the right of the plot.

An example, with  $HR_{ms}$  hardness ratio plotted versus X-ray to optical flux ratio, is shown in the upper panel of Figure 1. One can see a clear separation between AGN and HM-STAR/LM-STAR/YSO while other types of sources are overlapping, requiring an investigation of different sets of features to distinguish between them. Another example, in the lower panel of Figure 1, shows the  $BP-H$  color against  $G-W2$  color for AGN in red and HM-STAR in green. A subset of HM-STAR with bluer colors compared to other HM-STAR and AGN is selected by the *lasso* tool marked by highlighted cyan circles and shaded region will remain highlighted after changing to other combination of features plotted.

<sup>5</sup> described in detail in the CSC 2.0 website.

<sup>6</sup> The conversion for both  $P_{intra}$  and  $P_{inter}$  shown in the plotting tool is designed to emphasize the extremely variable sources with variability probability larger than 0.9 where the most variable sources with probability of 1 correspond to the value of 3 after the conversion.

<sup>7</sup> <https://bokeh.org>

## 5. SUMMARY

We provide an online tool, based on previously published X-ray source classifications and data from CSC 2.0 and multiple all-sky surveys, to visualize MW properties of X-ray sources with known classes. We ask anyone who will be using this tool in their work to cite this publication.

Support for this work was provided by NASA through CXO Awards AR8-19009B, AR9-20005A, AR0-21007X, and NASA ADAP award 80NSSC19K0576. JH acknowledges support from an appointment to the NASA Postdoctoral Program at the Goddard Space Flight Center, administered by the USRA through a contract with NASA.

## REFERENCES

- Clark, J. S., Munro, M. P., Negueruela, I., et al. 2008, *A&A*, 477, 147. doi:10.1051/0004-6361:20077186
- Cutri, R. M., Wright, E. L., Conrow, T., et al. 2021, *VizieR Online Data Catalog*, II/328
- Delgado, A. J., Alfaro, E. J., & Yun, J. L. 2011, *A&A*, 531, A141
- DeWitt, C., Bandyopadhyay, R. M., Eikenberry, S. S., et al. 2010, *ApJ*, 721, 1663. doi:10.1088/0004-637X/721/2/1663
- Downes, R. A., Webbink, R. F., Shara, M. M., et al. 2001, *PASP*, 113, 764
- Evans, I. N., Primini, F. A., Miller, J. B., et al. 2020, American Astronomical Society Meeting Abstracts #235
- Gaia Collaboration, Brown, A. G. A., Vallenari, A., et al. 2020, arXiv:2012.01533
- Giardino, G., Favata, F., Micela, G., et al. 2007, *A&A*, 463, 275
- Kargaltsev, O., Schmitt, B. M., Pavlov, G. G., et al. 2012, *ApJ*, 745, 99
- Laycock, S., Grindlay, J., van den Berg, M., et al. 2005, *ApJL*, 634, L53
- Lin, D., Webb, N. A., & Barret, D. 2012, *ApJ*, 756, 27
- Liu, Q. Z., van Paradijs, J., & van den Heuvel, E. P. J. 2006, *A&A*, 455, 1165
- Liu, Q. Z., van Paradijs, J., & van den Heuvel, E. P. J. 2007, *A&A*, 469, 807
- Manchester, R. N., Hobbs, G. B., Teoh, A., et al. 2005, *AJ*, 129, 1993
- Marocco, F., Eisenhardt, P. R. M., Fowler, J. W., et al. 2021, *ApJS*, 253, 8
- Megeath, S. T., Gutermuth, R., Muzerolle, J., et al. 2012, *AJ*, 144, 192
- Ozawa, H., Grosso, N., & Montmerle, T. 2005, *A&A*, 429, 963
- Povich, M. S., Smith, N., Majewski, S. R., et al. 2011, *ApJS*, 194, 14
- Rebull, L. M., Koenig, X. P., Padgett, D. L., et al. 2011, *ApJS*, 196, 4
- Rivera Sandoval, L. E., van den Berg, M., Heinke, C. O., et al. 2018, *MNRAS*, 475, 4841
- Schlafly, E. F., Meisner, A. M., & Green, G. M. 2019, *ApJS*, 240, 30
- Skiff, B. A. 2014, *VizieR Online Data Catalog*, B/mk
- Skrutskie, M. F., Cutri, R. M., Stiening, R., et al. 2006, *AJ*, 131, 1163
- Strader, J., Swihart, S., Chomiuk, L., et al. 2019, *ApJ*, 872, 42
- Tomsick, J. A., Bodaghee, A., Chaty, S., et al. 2020, *ApJ*, 889, 53
- van der Hucht, K. A. 2001, *NewAR*, 45, 135
- Vats, S. & van den Berg, M. 2017, *ApJ*, 837, 130.
- Véron-Cetty, M.-P. & Véron, P. 2010, *A&A*, 518, A10

## X-ray and multiwavelength properties of classified sources from CSC v.2

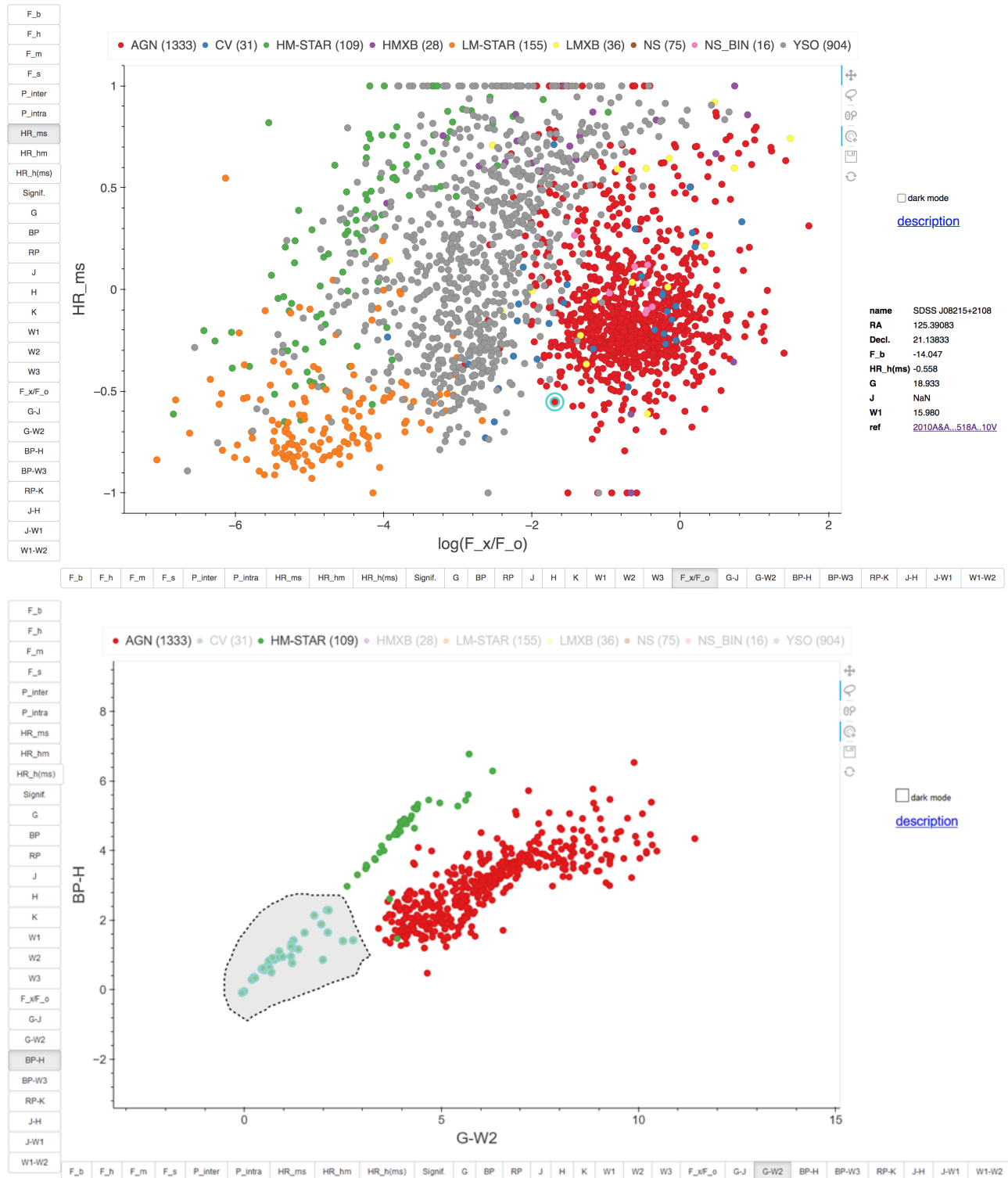


**Figure 1.** The upper panel shows a screenshot from the interactive visualization tool, available at <https://home.gwu.edu/~kargaltsev/XCLASS/>, of  $HR_{ms}$  hardness ratio versus X-ray to optical flux ratio for all nine classes of sources. The lower panel shows another screenshot of  $BP-H$  color versus  $G-W2$  color for AGNs in red and HM-STARS in green while a group of HM-STARS (within the shaded area) is selected by the *lasso* tool.